

Optimized tri-band MIMO antenna design for 6G terahertz applications and future connectivity

Jamal Hossain Nirob¹, Kamal Hossain Nahin¹, Md. Ashraful Haque¹, Redwan A. Ananta¹, Narinderjit Singh Sawaran Singh², Md. Kawsar Ahmed¹, Md. Sharif Ahammed¹, Liton Chandra Paul³

¹Department of Electrical and Electronic Engineering, Daffodil International University, Daffodil Smart City, Bangladesh

²Faculty of Data Science and Information Technology, INTI International University, Nilai, Malaysia

³Department of Electrical, Electronic and Communication Engineering, Pabna University of Science and Technology, Pabna, Bangladesh

Article Info

Article history:

Received Aug 12, 2024

Revised Dec 25, 2024

Accepted Jan 23, 2025

Keywords:

6G communication
Industrial and innovation
Multiple input multiple output
Resistor, inductor, and capacitor
Terahertz
Tri-band

ABSTRACT

This paper presents an industrial and innovation rectangular-shaped multiple input multiple output (MIMO) antenna designed for terahertz (THz) frequency applications, specifically targeting 6G communication. The proposed antenna achieves triple-band operation at 3.62 THz, 6.248 THz, and 7.613 THz by incorporating four T-shaped slots. It is designed on a polyimide substrate with a dielectric constant of 3.5 and a tangent loss of 0.0027, with dimensions of 80 μm by 180 μm and a thickness of 11 μm . The patch and the ground plane are constructed from copper, ensuring robust performance. The antenna provides bandwidths of 0.7 THz, 2.2 THz, and 1.1 THz, with isolation levels exceeding -31.3 dB. It achieves a peak gain of 14.3 dB and a high efficiency of 94%, demonstrating its potential for high-performance THz applications. MIMO performance parameters, such as the envelope correlation coefficient (ECC), diversity gain (DG), mean effective gain (MEG), and total active reflection coefficient (TARC), exhibit excellent agreement with theoretical values. The design is further validated through simulations using computer simulation technology (CST) and a circuit model in advanced design system (ADS). The results of these tests mirrored those of the CST simulations, confirming the reliability of future 6G THz communication systems.

This is an open access article under the [CC BY-SA](https://creativecommons.org/licenses/by-sa/4.0/) license.



Corresponding Author:

Narinderjit Singh Sawaran Singh

Faculty of Data Science and Information Technology, INTI International University

Persiaran Perdana BBN, Putra Nilai, Nilai 71800, Negeri Sembilan, Malaysia

Email: narinderjits.sawaran@newinti.edu.my

1. INTRODUCTION

The evolution of wireless communication technology is rapidly progressing towards 6G, aiming to fulfil the increasing demand for high data rates, ultra-low latency, and massive connectivity. A key enabler for 6G technology is the utilization of terahertz (THz) frequency bands, which offer unprecedented bandwidth capabilities for short-range wireless communication [1]. THz communication stands out because it can provide extremely high data transfer rates, making it ideal for applications such as high-definition video streaming, augmented reality, and advanced IoT networks [2]. THz frequencies, typically ranging from 0.1 to 10 THz, offer significantly higher bandwidth than traditional microwave and millimeter-wave frequencies [3]. This higher bandwidth translates to greater data transfer rates, which is essential for meeting future wireless applications' performance requirements. Short-range wireless communication, which involves distances typically within a few meters, benefits immensely from THz technology because it can handle large

volumes of data with minimal latency [4]. However, using THz frequencies introduces challenges, such as high path loss, limited penetration capabilities, and susceptibility to atmospheric absorption. It is imperative that these issues be addressed for practically deploying THz communication systems [5].

Incorporating multiple input multiple output (MIMO) technology with THz communication further enhances performance by leveraging spatial diversity to improve signal strength and data throughput [6]. Simultaneous transmission and reception of various data streams is made possible by MIMO technology, which use a number of antennas on both the transmitter and the receiver. This spatial multiplexing capability significantly increases wireless communication systems' capacity and spectral efficiency [7]. The combination of THz communication with MIMO systems is poised to overcome the limitations of traditional communication systems by significantly increasing capacity and spectral efficiency [8]. This synergy is crucial for realizing the full potential of 6G technology, as it supports a wide range of applications requiring ultra-fast and reliable wireless connections [9]. The integration of THz communication and MIMO technology represents a significant advancement in wireless communication. As the demand for higher data rates and more reliable connections continues to grow, system development will play a critical role in shaping the future of 6G technology, ensuring seamless connectivity and enhanced user experiences in short-range wireless communication environments [10].

A comparative study of several MIMO antenna designs is shown in Table 1, focusing on their fundamental parameters and performance metrics. The proposed antenna design stands out with its remarkable performance across these parameters, showcasing significant advancements in antenna technology and setting a new standard for comparison.

Bandwidth values show considerable variation, with measurements including 0.05 THz, 0.114 THz, 0.038 THz, 0.3 THz, 0.78 THz, and 0.4 THz at [11], [12]. In contrast, the proposed design achieves significantly broader bandwidths of 0.7 THz, 2.2 THz, and 1.1 THz at its three resonance frequencies of 3.62 THz, 6.248 THz, and 7.61 THz, respectively. The gain values reported in the references are 11.67 dB, 4.4 dB, 5 dB, 10 dB, 4.4 dB, and 5.49 dB [11], [12]. The proposed design, however, achieves substantially higher gains of 13.5 dB, 14.3 dB, and 13.9 dB at its three resonance frequencies. Isolation is another critical factor in which the proposed design excels. The referenced antennas exhibit isolation values of -25 dB, -17 dB, -17 dB, -35 dB, -20 dB, and -25 dB at [11], [12]. In comparison, the proposed antenna achieves isolation levels of -33.32 dB, -30.01 dB, and -35.27 dB across its three bands. In terms of efficiency, the proposed antenna also outperforms the referenced designs. The efficiencies reported in the references are 76.45%, 94%, 60%, 96%, and 85.24% [11]-[14]. The proposed antenna achieves efficiencies of 93.77%, 95.2%, and 93.79% at its three operating frequencies. The suggested MIMO antenna performed exceptionally well compared to other options, with an ECC <0.0007 and a diversity gain (DG) above 9.996. Notably, whereas references [14], [15], used resistor, inductor, and capacitor (RLC) circuits, the suggested antenna incorporates RLC components to evaluate its electromagnetic behaviour, distinguishing it and emphasizing its novel approach. These attributes together demonstrate the suggested antenna's ability to lead the field of antenna technology and drive future developments, making it the best of the compared designs.

Table 1. Performance metrics comparison of proposed MIMO antenna and existing designs

Ref	Resonance (THz)	BW (THz)	Isolation (dB)	Gain (dB)	Efficiency (%)	ECC, DG (dB)	Substrate material	Port	RLC
[11]	0.654	0.05	-25	11.67	76.45%	0.003, 9.99	polyimide	-	No
[16]	-	0.114	-17	4.4	94	0.006, 9.97	Rogers RO4835-T	4	No
[13]	2.3, 3.2, 4.5	0.038, 0.043, 0.06	-17, -30, -23	5	60%	0.2, 10	Polyimide	2	No
[15]	1.9	0.3	-35	10	-	0.00002, 3/9.99	Polyimide	2	Yes
[14]	2.2	0.78	-20	4.4	96	0.006, 9.9998	Polyimide	2	Yes
[12]	-	0.4	-25	5.49	85.24	0.015/ 9.99	Polyimide	2	No
Proposed	3.62, 6.24, 7.61	0.7, 2.2, 1.1	-33.32, -30.01, -35.27	13.5, 14.3, 13.9	93.77, 95.2, 93.79	0.0007, 9.996	Polyimide	2	Yes

2. ITERATIVE DESIGN AND ANALYSIS OF THE SINGLE-ELEMENT ANTENNA

In our endeavour to engineer a cutting-edge antenna for THz applications, we meticulously designed a single-element antenna, refining its architecture through three progressive stages to attain optimal

performance. The final design of this antenna is presented in Figure 1, which shows Figure 1(a) presenting a 3D view, Figure 1(b) showcasing the side view, Figure 1(c) displaying the front view, and Figure 1(d) highlighting the back view.

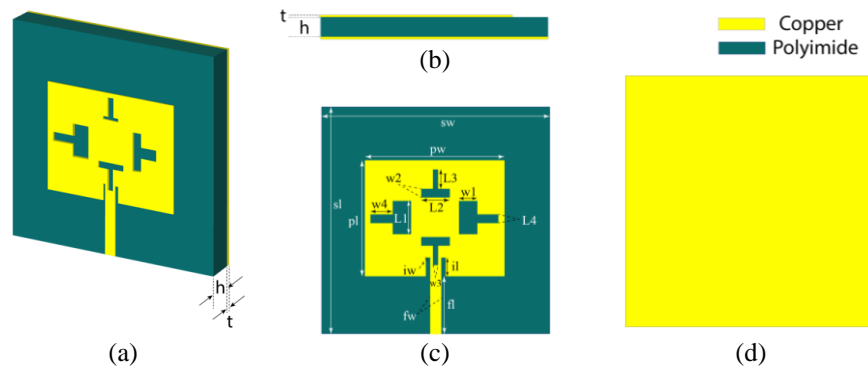


Figure 1. Antenna configuration; (a) 3D perspective view, (b) side view, (c) front view, and (d) back view

Polyimide is chosen as the substrate due to its superior dielectric properties, boasting a dielectric constant of 3.5 and a low-loss tangent of 0.0027 [17]. This strategic choice reassures us of the robustness and reliability of our design. Copper was employed for both the patch and ground elements to maximize conductivity, thereby enhancing signal grounding and radiation efficiency. The design consistently featured a full ground plane, ensuring robust performance. In (1) and (2) were used to calculate the antenna's measurements [18].

$$W = \frac{c}{2f} \times \sqrt{\frac{2}{\epsilon_r + 1}} \quad (1)$$

$$L = \frac{c}{(2f\sqrt{\epsilon_{\text{eff}}})} - 2 \times \Delta L \quad (2)$$

The antenna's reflection coefficient across each design stage is demonstrated in Figure 2(a), while Figure 2(b) depicts the corresponding gain. In the initial design, a facile rectangular patch antenna with a feedline and two symmetrical rectangular slots was used. This configuration produced two resonance frequencies, but the performance was subpar, particularly in return loss, and gain. To address these issues, further design refinements were pursued in the next stage. Building upon the foundational design, in the second stage two rectangular slots were added above and below the central section of the patch, and insets were introduced on both sides of the feedline. This refinement resulted in dual-band frequencies at 3.81 THz and 6.5 THz, with improved return losses of -21.44 dB and -34.36 dB, respectively. The gain also showed notable improvement, although there remained potential for further optimization. In the final design, we incorporated small extensions, akin to arms, on the sides of the rectangular slots. This enhancement resulted in three distinct resonance frequencies at 3.75 THz, 6.38 THz, and 7.74 THz, with impressive return losses of -26.54 dB, -50.5 dB, and -38.5 dB, respectively. The antenna's peak gain was recorded at 11.7 dB, underscoring its reliability and efficiency. Additionally, the antenna achieved substantial bandwidths of 0.5 THz, 1 THz, and 0.63 THz at its three operating frequencies. These exceptional performance characteristics underscore the antenna's viability for integration into advanced 6G communication systems.

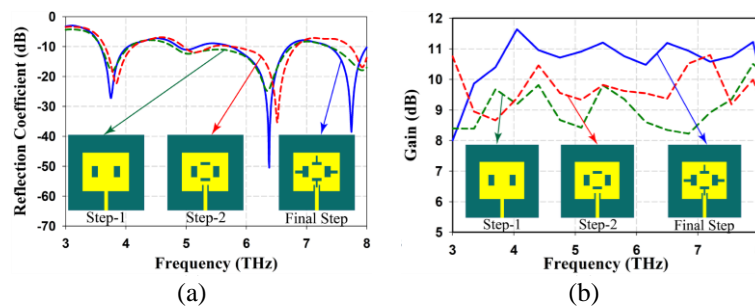


Figure 2. Performance analysis of the single-element antenna design; (a) S11 comparison and (b) Gain comparison

3. DESIGN AND ANALYSIS OF THE MIMO ANTENNA

MIMO antennas offer substantial advantages over single-element designs, including enhanced system capacity, improved data throughput, and superior signal quality. MIMO antennae can deliver higher performance by exploiting spatial diversity and reducing interference. Especially in complex communication environments [19].

In this section, we describe the progression of a 2-port MIMO antenna, evolving from a single-element design to enhance overall performance. Figure 3(a) illustrates the MIMO antenna configuration, featuring two elements placed side by side with a 180-degree orientation relative to each other. The antennas are spaced $40 \mu\text{m}$ apart edge-to-edge, within an overall dimension of $80 \times 180 \mu\text{m}$. This arrangement is designed to maximize spatial diversity and minimize mutual coupling, thereby optimizing signal quality and reliability. Following implementing the MIMO configuration, we identified three distinct resonance frequencies at 3.62 THz, 6.24 THz, and 7.61 THz. The bandwidths achieved are 0.7 THz, 2.2 THz, and 1.1 THz at its three operating frequencies, as displayed in Figure 3(b). Additionally, Figure 3(c) highlights a maximum gain of 14.3 dB. Figures 3(b) and (c) provide a comparative analysis of return loss and gain respectively between the single-element and MIMO antenna. These figures demonstrate that the MIMO antenna offers markedly superior performance compared to the single-element antenna.

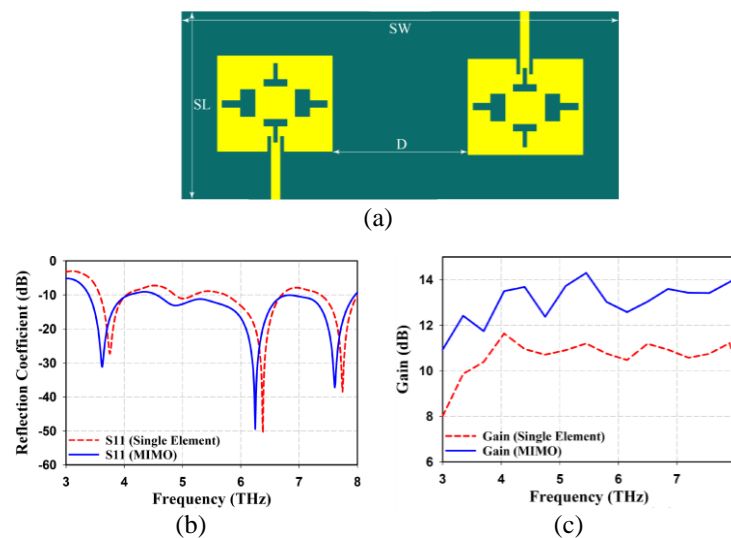


Figure 3. Performance comparison of single-element and MIMO antenna; (a) MIMO antenna design, (b) S11 parameter comparison, and (c) gain comparison

These values represent the ideal setting of the antenna, $sw=70 \mu\text{m}$, $sl=80 \mu\text{m}$, $pw=45 \mu\text{m}$, $pl=40 \mu\text{m}$, $L1=12 \mu\text{m}$, $L2=10 \mu\text{m}$, $L3=7 \mu\text{m}$, $L4=3 \mu\text{m}$, $w1=6 \mu\text{m}$, $w2=3 \mu\text{m}$, $w3=2 \mu\text{m}$, $w4=8 \mu\text{m}$, $iw=1 \mu\text{m}$, $il=6 \mu\text{m}$, $fl=20 \mu\text{m}$, $fw=4 \mu\text{m}$, $h=11 \mu\text{m}$, $t=0.5 \mu\text{m}$, $D=40 \mu\text{m}$, $SW=180 \mu\text{m}$, and $SL=80 \mu\text{m}$.

4. RESULTS ANALYSIS OF THE RECOMMENDED MIMO ANTENNA

4.1. Reflection coefficient and transmission coefficient analysis

The reflection coefficient measures how much power is reflected back from the antenna, with lower values indicating better impedance matching [20]. Figure 4(a) illustrates that the proposed MIMO antenna achieves triple-band operation, resonating at three distinct frequencies: 3.62 THz, 6.248 THz, and 7.61 THz. The return losses at these resonance frequencies are -31.114 dB, -49.45 dB, and -37.22 dB, respectively, indicating excellent impedance matching. The first band operates between 3.39 THz and 4.09 THz, providing a bandwidth of 0.7 THz. The second band spans from 4.56 THz to 6.76 THz, resulting in a high bandwidth of 2.2 THz. The third band operates between 6.76 THz and 7.86 THz, with a bandwidth of 1.1 THz. These wide bandwidths ensure the antenna's capability to support a broad range of frequencies, making it highly suitable for advanced THz applications.

Isolation or transmission coefficient is crucial in MIMO systems, showing how much the antenna parts interact with one another [21]. The proposed antenna achieves a very high isolation value of -30.01 dB (shown in Figure 4(b)). Which is excellent and suggests that the antenna elements are well-isolated, reducing cross-talk and enhancing overall system performance [22].

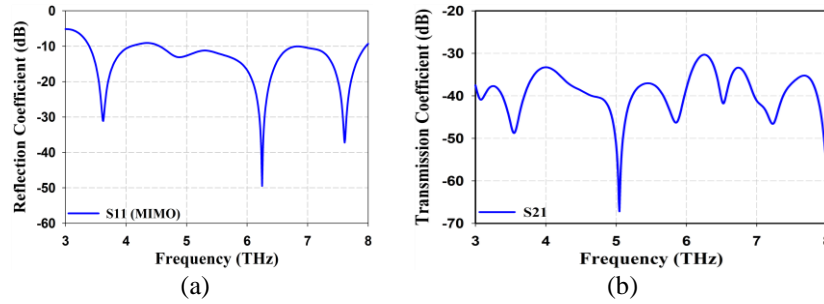


Figure 4. Performance analysis of the proposed MIMO antenna; (a) reflection and (b) transmission coefficient

4.2. Gain and efficiency

Gain and efficiency are essential metrics for evaluating antenna performance. Gain refers to the ability of an antenna to direct radiated energy in a particular direction, which enhances signal strength and improves communication range [23], [24]. Efficiency represents the effectiveness of an antenna in converting input power into radiated energy with minimal losses [25]. Figure 5 depicts a plot of the simulated gain and Efficiency of the suggested antenna. The proposed antenna achieves maximum gains of 13.5 dB, 14.3 dB, and 13.9 dB at the respective bands of 3.62 THz, 6.248 THz, and 7.61 THz. These high gain values indicate the antenna's ability to direct energy efficiently, which is crucial for long-distance communication. Additionally, the antenna maintains high efficiencies of 92%, 94%, and 93% at the three respective bands. This high efficiency indicates that the antenna effectively converts input power into radiated energy with minimal losses, optimizing overall performance [26].

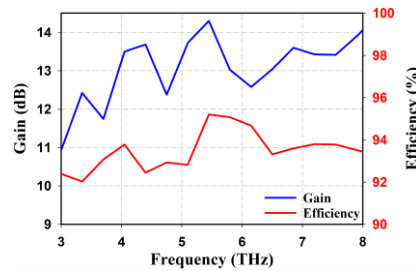


Figure 5. Gain and efficiency of the proposed THz MIMO antenna

4.3. Diversity performance analysis

The diversity performance of the proposed antenna is assessed using the envelope correlation coefficient (ECC), DG, mean effective gain (MEG), total active reflection coefficient (TARC) [27]. The ECC indicates how similar or different the signals received by the different antennas are. The value of ECC can be figured out by using the expression shown in (3) [28]:

$$\frac{|\int_{4\pi} [E_1(\theta, \varphi) * E_2(\theta, \varphi)] d\Omega|^2}{\int_{4\pi} |E_1(\theta, \varphi)|^2 d\Omega \int_{4\pi} |E_2(\theta, \varphi)|^2 d\Omega} \quad (3)$$

The antenna achieves an ECC value of 0.00004, which is exceptionally low and desirable, as shown in Figure 6(a). This low ECC enhances the antenna's ability to provide multiple independent signal paths, improving signal quality and reliability.

The DG, which measures the improvement in signal quality achieved through diversity, is nearly ideal at 9.99999, as shown in the same figure of ECC (Figure 6(a)). The value of DG can be determined by using the equation provided here [29].

$$DG = 10\sqrt{1 - ECC^2} \quad (4)$$

This high DG value, confirms the excellent diversity performance of the antenna, ensuring robust communication even in challenging environments.

In Figure 6(b), the TARC plot shows weighty dips at the operational frequencies (3.62 THz, 6.248 THz, and 7.613 THz), signifying good impedance matching and low reflection, critical for efficient antenna performance in 6G THz applications. In (3) can be utilised to ascertain this [30].

$$TARC = \frac{\sqrt{(|S_{xx}|+|S_{xy}|)^2+(|S_{yx}|+|S_{yy}|)^2}}{\sqrt{4}} \quad (5)$$

In Figure 6(c), the MEG plot for the two MIMO antenna ports (MEG 1 and MEG 2) are meticulously associated and relatively constant across the frequency range, prominence well-adjusted performance and good signal response, important for accomplishing high DG and low correlation in MIMO systems. It can be mathematically represented as (6) and (7) [31]:

$$k = \min\left(\frac{MEG_1}{MEG_2}, \frac{MEG_2}{MEG_1}\right) \quad (6)$$

$$MEG_i = 0.5 \left[1 - \sum_{j=1}^N S_{ij}\right] \quad (7)$$

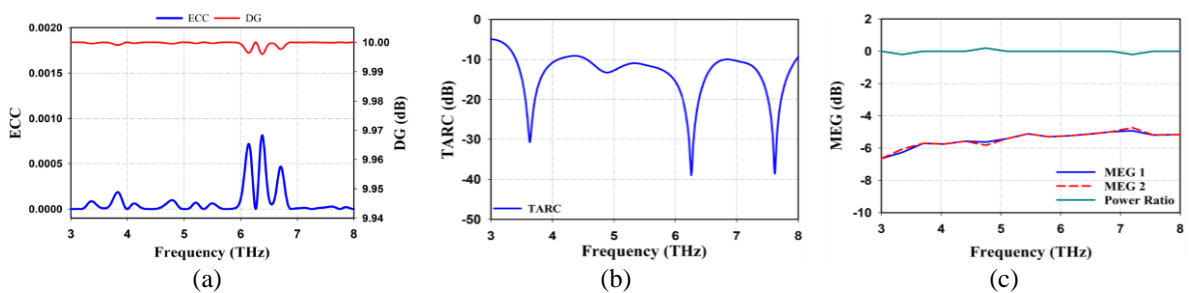


Figure 6. Diversity performance; (a) ECC and DG, (b) TARC, and (c) MEG of the MIMO antenna

4.4. Radiation pattern

The radiation pattern analysis of the proposed antenna at 6.5 THz, illustrated in Figure 7, reveals notable E-field and H-field characteristics. At $\phi=0^\circ$, the E-field displays a main lobe magnitude of 11.1 dBV/m with a 3 dB beamwidth of 41.7 degrees, whereas the H-field shows a main lobe magnitude of -37.9 dBA/m and a beamwidth of 17.3 degrees. In the $\phi=90^\circ$ plane, the E-field's main lobe magnitude is 8.73 dBV/m with a 3 dB beamwidth of 15.6 degrees, while the H-field presents a magnitude of -26.8 dBA/m and a beamwidth of 33.5 degrees. Additionally, for $\theta=90^\circ$, the E-field achieves a main lobe magnitude of 24.8 dBV/m with a beamwidth of 28.5 degrees, and the H-field has a magnitude of -39.1 dBA/m with a 3 dB beamwidth of 8.7 degrees. These patterns, demonstrate the antenna's capability to deliver efficient directional radiation across different planes at its operating frequency [32].

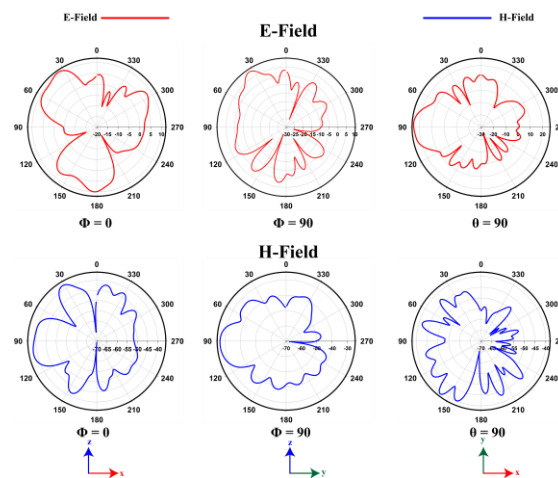


Figure 7. Simulated radiation pattern

5. EQUIVALENT CIRCUIT MODELING

To advance our antenna technology, we meticulously analyzed the electromagnetic behavior of our antenna using an R-L-C circuit model. The R-L-C parameters were precisely extracted from CST Studio simulations, which we further refined through circuit simulations in Agilent advanced design system (ADS), enabling a comprehensive performance assessment [33]. During the RLC equivalent circuit design, we employed a trial-and-error approach using ADS software, iteratively adjusting the RLC parameters to achieve optimal results.

In our antenna design process, we identified that the three resonance frequencies were primarily influenced by the four T-shaped slots. Consequently, we designed a plus-shaped circuit corresponding to these slots. Each T-shaped slot was modeled as a parallel circuit of resistance (R), capacitance (C), and inductance (L), connected in series with another resistance (R). These circuits were crucial in determining the antenna's resonance frequencies. Additionally, the capacitance between two adjacent T-shaped slots was represented by a series circuit of two capacitors. The feedline was also modeled with specific resistance (Rx), capacitance (Cx), and inductance (Lx) parameters to accurately reflect its electrical properties. By integrating these circuit elements, we constructed a model that faithfully represented the behavior of our single-element antenna. We then extended this model to a MIMO antenna configuration, as shown in Figure 8, using the single-element circuit as a foundation. To adapt to the MIMO setup, we incorporated the mutual impedance between antenna elements using a parallel circuit composed of L5 and C9. This approach optimized the performance evaluation. We validated the R-L-C circuit model through simulations in Agilent ADS, ensuring its alignment with our antenna design. To confirm its precision, we compared the CST simulation results with those obtained from the circuit simulation, focusing specifically on the S11 parameter. Figure 9 illustrates this comparison, providing a thorough evaluation of our R-L-C circuit model's accuracy in representing the antenna's behavior.

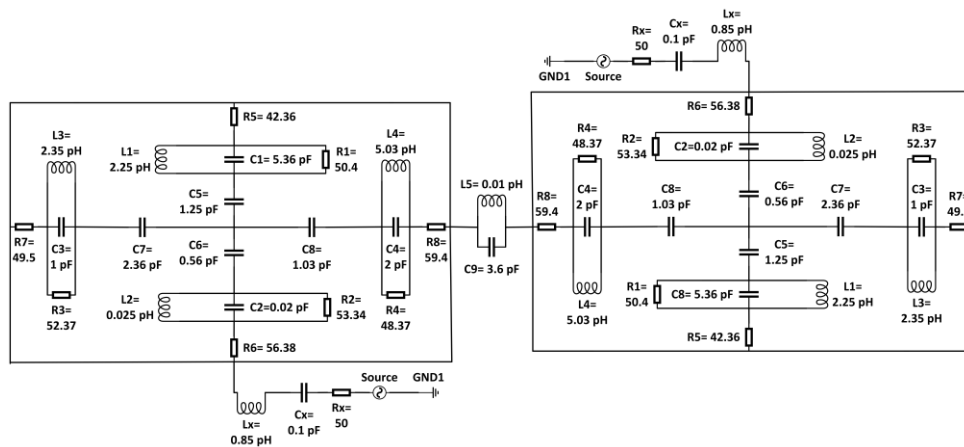


Figure 8. RLC equivalent circuit diagram for the suggested MIMO antenna

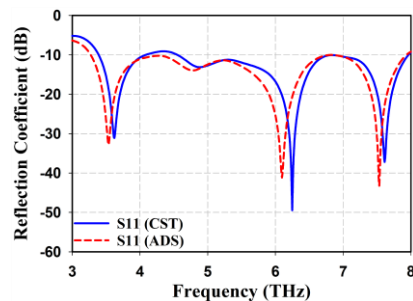


Figure 9. Comparative plot of S11 parameter from CST and ADS simulations

6. CONCLUSION

This research has thoroughly investigated a novel MIMO antenna adapted for THz applications, utilizing a range of analytical methods, including the creation of an RLC-equivalent circuit model. The performance of the proposed antenna was meticulously evaluated through both ADS and CST simulations,

demonstrating a remarkable consistency in bandwidth across these platforms. The antenna's design showcases exceptional performance characteristics, including broad bandwidth, high isolation, significant gain, and impressive efficiency. The isolation parameter effectively reduces mutual coupling among antenna elements, which is crucial for maintaining optimal performance in a MIMO system. Additionally, the antenna excels in diversity performance, evidenced by a very low ECC and an almost perfect DG, indicating its potential to deliver high-quality and reliable communication. The consistency of results obtained from different simulation environments underscores the robustness and reliability of the proposed design. Overall, the research validates the effectiveness of the MIMO antenna for advanced THz communication systems and provides a solid foundation for further developments and practical applications in next-generation communication technologies. This study not only highlights the antenna's impressive performance metrics but also provides precious insights into the design and evaluation of high-frequency communication systems.

ACKNOWLEDGEMENT

The authors acknowledge the collaboration of the Department of Electrical and Electronic Engineering and the Faculty of Graduate Studies at Daffodil International University in Bangladesh.

REFERENCES

- [1] C. M. Krishna, S. Das, A. Nella, S. Lakrit, and B. T. P. Madhav, "A Micro-Sized Rhombus-Shaped THz Antenna for High-Speed Short-Range Wireless Communication Applications," *Plasmonics*, vol. 16, no. 6, pp. 2167–2177, Dec. 2021, doi: 10.1007/s11468-021-01472-z.
- [2] F. Guo, F. R. Yu, H. Zhang, X. Li, H. Ji, and V. C. M. Leung, "Enabling Massive IoT Toward 6G: A Comprehensive Survey," *IEEE Internet Things J.*, vol. 8, no. 15, pp. 11891–11915, Aug. 2021, doi: 10.1109/JIOT.2021.3063686.
- [3] M. A. Jamshed, A. Nauman, M. A. B. Abbasi, and S. W. Kim, "Antenna Selection and Designing for THz Applications: Suitability and Performance Evaluation: A Survey," *IEEE Access*, vol. 8, pp. 113246–113261, 2020, doi: 10.1109/ACCESS.2020.3002989.
- [4] N. S. Asaad, A. M. Saleh, and M. A. Alzubaidy, "Analyzing Performance of THz Band Graphene-Based MIMO Antenna for 6G Applications," *JTIT*, Jul. 2024, doi: 10.26636/jtit.2024.3.1518.
- [5] J. Tan and L. Dai, "THz Precoding for 6G: Challenges, Solutions, and Opportunities," *IEEE Wireless Commun.*, vol. 30, no. 4, pp. 132–138, Aug. 2023, doi: 10.1109/MWC.015.2100674.
- [6] M. H. Loukil, H. Sareddeen, M.-S. Alouini, and T. Y. Al-Naffouri, "Terahertz-Band MIMO Systems: Adaptive Transmission and Blind Parameter Estimation," *IEEE Commun. Lett.*, vol. 25, no. 2, pp. 641–645, Feb. 2021, doi: 10.1109/LCOMM.2020.3029632.
- [7] P. Sharma, R. N. Tiwari, P. Singh, P. Kumar, and B. K. Kanaujia, "MIMO Antennas: Design Approaches, Techniques and Applications," *Sensors*, vol. 22, no. 20, p. 7813, Oct. 2022, doi: 10.3390/s22207813.
- [8] K. Ramesh Chandra and S. Borugadda, "An effective combination of terahertz band NOMA and MIMO system for power efficiency enhancement," *Int J Commun.*, vol. 35, no. 11, p. e5187, Jul. 2022, doi: 10.1002/dac.5187.
- [9] K. M. Luk *et al.*, "A microfabricated low-profile wideband antenna array for terahertz communications," *Sci Rep.*, vol. 7, no. 1, p. 1268, Apr. 2017, doi: 10.1038/s41598-017-01276-4.
- [10] M. Alsabah *et al.*, "6G Wireless Communications Networks: A Comprehensive Survey," *IEEE Access*, vol. 9, pp. 148191–148243, 2021, doi: 10.1109/ACCESS.2021.3124812.
- [11] R. Pant and L. Malviya, "Terahertz MIMO antenna array for future generation of wireless applications," *Frequenz*, vol. 78, no. 5–6, pp. 271–280, Jun. 2024, doi: 10.1515/freq-2023-0203.
- [12] K. V. Babu, S. Das, G. N. J. Sree, B. T. P. Madhav, S. K. K. Patel, and J. Parmar, "Design and optimization of micro-sized wideband fractal MIMO antenna based on characteristic analysis of graphene for terahertz applications," *Opt Quant Electron.*, vol. 54, no. 5, p. 281, May 2022, doi: 10.1007/s11082-022-03671-2.
- [13] K. Vijayalakshmi, C. S. K. Selvi, and B. Sapna, "Novel tri-band series fed microstrip antenna array for THz MIMO communications," *Opt Quant Electron.*, vol. 53, no. 7, p. 395, Jul. 2021, doi: 10.1007/s11082-021-03065-w.
- [14] A. Kumar, D. Saxena, P. Jha, and N. Sharma, "Compact two-port antenna with high isolation based on the defected ground for THz communication," *Results in Optics*, vol. 13, p. 100522, Dec. 2023, doi: 10.1016/j.rio.2023.100522.
- [15] S. A. Khaleel, E. K. I. Hamad, N. O. Parchin, and M. B. Saleh, "Programmable Beam-Steering Capabilities Based on Graphene Plasmonic THz MIMO Antenna via Reconfigurable Intelligent Surfaces (RIS) for IoT Applications," *Electron.*, vol. 12, no. 1, p. 164, Dec. 2022, doi: 10.3390/electronics12010164.
- [16] T. Okan, "High efficiency unslotted ultra-wideband microstrip antenna for sub-terahertz short range wireless communication systems," *Optik*, vol. 242, p. 166859, Sep. 2021, doi: 10.1016/j.ijleo.2021.166859.
- [17] D. Ziani, M. Belkheir, M. Rouissat, and A. Mokaddem, "Design optimization for improving the performance of rectangular antennas using polyimide (PI) and liquid crystal (LC) polymers substrates," *Polym. Bull.*, vol. 81, no. 9, pp. 8447–8469, Jun. 2024, doi: 10.1007/s00289-023-05114-8.
- [18] M. F. Ali, T. Jiya, K. R. Singh, and G. Varshney, "Terahertz antenna with controllable and tunable filtering characteristics," *Micro Nanostruct.*, vol. 174, p. 207476, Feb. 2023, doi: 10.1016/j.micrna.2022.207476.
- [19] G. Saxena *et al.*, "Metasurface inspired wideband high isolation THz MIMO antenna for nano communication including 6G applications and liquid sensors," *Nano Commun. Netw.*, vol. 34, p. 100421, Dec. 2022, doi: 10.1016/j.nancom.2022.100421.
- [20] L. C. Paul, M. A. Haque, M. A. Haque, M. M. U. Rashid, M. F. Islam, and M. M. Rahman, "Design a slotted metamaterial microstrip patch antenna by creating three dual isosceles triangular slots on the patch and bandwidth enhancement," in *2017 3rd Int. Conf. Electr. Inf. Commun. Technol. (EICT)*, Khulna: IEEE, Dec. 2017, pp. 1–6, doi: 10.1109/EICT.2017.8275143.
- [21] N. S. and S. V., "MIMO Antenna with Isolation Enrichment for 5G Mobile Information," *Mob. Inf. Syst.*, vol. 2022, pp. 1–14, Feb. 2022, doi: 10.1155/2022/1802352.
- [22] M. F. Ali and R. Bhattacharya, "Polarization-insensitive graphene-based THz absorber with ATA characteristics," *Phys. Scr.*, vol. 99, no. 1, p. 015501, Jan. 2024, doi: 10.1088/1402-4896/ad0fcc.

- [23] Md. A. Haque, L. C. Paul, R. Azim, Md. M. Mowla, A. Saleh, and Md. N. Hossain, "A Modified E-Shaped Microstrip Patch Antenna for C Band Satellite Applications," in *2019 IEEE Int. Conf. Signal Process. Inf. Commun. Syst. (SPICSCON)*, Dhaka, Bangladesh: IEEE, Nov. 2019, pp. 27–31, doi: 10.1109/SPICSCON48833.2019.9065126.
- [24] Md. A. Haque, M. A. Zakariya, L. C. Paul, D. Nath, P. Biswas, and R. Azim, "Analysis of Slotted E-shaped Microstrip Patch Antenna for Ku Band Applications," in *2021 IEEE 15th Malaysia Int. Conf. Commun. (MICC)*, Malaysia: IEEE, Dec. 2021, pp. 98–101, doi: 10.1109/MICC53484.2021.9642100.
- [25] Md. K. Ahmed *et al.*, "based performance estimation of a slotted inverted F-shaped tri-band antenna for satellite/mm-wave 5G application," *TELKOMNIKA (Telecommunication Computing Electronics and Control)*, vol. 22, no. 4, pp. 773-783, Aug. 2024, doi: 10.12928/telkomnika.v22i4.26028.
- [26] M. F. Ali and R. Bhattacharya, "Tunable high-gain graphene patch antenna for THz massive MIMO applications using FSS," *Opt Quant Electron*, vol. 55, no. 13, p. 1204, Dec. 2023, doi: 10.1007/s11082-023-05326-2.
- [27] S. Kareemulla and V. Kumar, "Diversity performance of band notched ultra-wideband MIMO antenna," *Optik*, vol. 272, p. 170128, Feb. 2023, doi: 10.1016/j.ijleo.2022.170128.
- [28] A. A. Althuwayb *et al.*, "Broadband, high gain 2×2 spiral shaped resonator based and graphene assisted terahertz MIMO antenna for biomedical and WBAN communication," *Wireless Netw.*, vol. 30, no. 1, pp. 495–515, Jan. 2024, doi: 10.1007/s11276-023-03494-3.
- [29] V. Sorathiya *et al.*, "Graphene-Based Log-Periodic Dipole Antenna-Shaped MIMO Antenna Structure for the Terahertz Frequency Spectrum," *Arab J Sci Eng*, vol. 49, no. 5, pp. 6391–6404, May 2024, doi: 10.1007/s13369-023-08235-4.
- [30] M. F. Ali, R. Bhattacharya, and G. Varshney, "Tunable four-port MIMO/self-multiplexing THz graphene patch antenna with high isolation," *Opt Quant Electron*, vol. 54, no. 12, p. 822, Dec. 2022, doi: 10.1007/s11082-022-04200-x.
- [31] M. F. Ali, A. Singh, P. Giri, and G. Varshney, "Graphene Supported Ultrathin VO₂ Resonators for Multifunctional THz Absorption," *IEEE Trans. Plasma Sci.*, vol. 52, no. 2, pp. 545–552, Feb. 2024, doi: 10.1109/TPS.2023.3342115.
- [32] M. M. Fakharian, "A graphene-based multi-functional terahertz antenna," *Optik*, vol. 251, p. 168431, Feb. 2022, doi: 10.1016/j.ijleo.2021.168431.
- [33] Md. A. Haque *et al.*, "Machine learning-based technique for resonance and directivity prediction of UMTS LTE band quasi Yagi antenna," *Heliyon*, vol. 9, no. 9, p. e19548, Sep. 2023, doi: 10.1016/j.heliyon.2023.e19548.

BIOGRAPHIES OF AUTHORS



Jamal Hossain Nirob    is a student in the Department of Electrical and Electronic Engineering (EEE) at Daffodil International University. His educational journey began at Maniknagar High School, where he successfully completed his Secondary School Certificate (SSC). Following that, he pursued higher studies at Ishwardi Government College, obtaining his Higher Secondary Certificate (HSC). With a strong enthusiasm for expanding communication technology, he has focused his research on wireless communication, specifically on microstrip patch antennas, terahertz antennas, and applications of 5G and 6G. He can be contacted at email: jamal33-1243@diu.edu.bd.



Kamal Hossain Nahin    currently pursuing a degree in Electrical and Electronic Engineering at Daffodil International University. His educational journey commenced at Ishwardi Govt College for Higher Secondary Certificate (HSC) and earlier at Maniknagar High School for Secondary School Certificate (SSC). Embarking on a journey as a budding researcher in the communication field, he is passionately immersed in exploring the realms of wireless communication. His focus lies in delving into the intricacies of wireless communication, particularly exploring microstrip patch antennas, terahertz antennas, and their potential applications in the future realms of 5G and 6G technologies. He can be contacted at email: kamal33-1242@diu.edu.bd.



Md. Ashraful Haque    is doing Ph.D. at the Department of Electrical and Electronic Engineering, Universiti Teknologi PETRONAS, Malaysia. He got his B.Sc. in Electronics and Electronic Engineering (EEE) from Bangladesh's Rajshahi University of Engineering and Technology (RUET) and his M.Sc. in the same field from Bangladesh's Islamic University of Technology (IUT). He is currently on leave from Daffodil International University (DIU) in Bangladesh. His research interest includes microstrip patch antenna, sub 6 5G application, and supervised regression model machine learning on antenna design. He can be contacted at email: limon.ashraf@gmail.com.



Redwan A. Ananta    has accomplished his undergraduate studies in the field of Electrical and Electronics at Daffodil International University. He completed his higher secondary education at Adamjee Cantonment College. His research focus encompasses wireless communication, specifically microstrip patch antenna, terahertz antenna, 5G, and 6G applications. He can be contacted at email: redwan33-1145@diu.edu.bd.



Narinderjit Singh Sawaran Singh    is an Associate Professor in INTI International University, Malaysia. He graduated from the Universiti Teknologi PETRONAS (UTP) in 2016 with Ph.D. in Electrical and Electronic Engineering specialized in Probabilistic methods for fault tolerant computing. Currently, he is appointed as the research cluster head for computational mathematics, technology and optimization which focuses on the areas like pattern recognition and symbolic computations, game theory, mathematical artificial intelligence, parallel computing, expert systems and artificial intelligence, quality software, information technology, exploratory data analysis, optimization algorithms, stochastic methods, data modelling, and computational intelligence-swarm intelligence. He can be contacted at email: narinderjits.sawaran@newinti.edu.my.



Md. Kawsar Ahmed    is currently pursuing his studies in the field of Electrical and Electronic Engineering at Daffodil International University. He successfully finished his Higher Secondary education at Agricultural University College, Mymensingh. He is presently employed as an Assistant Administrative Officer at the Office of Students' Affairs at Daffodil International University (DIU) in Bangladesh. The areas of his research focus encompassed microstrip patch antennas, terahertz antennas, and applications related to 4G and 5G technologies. He can be contacted at email: kawsar33-1241@diu.edu.bd.



Md. Sharif Ahammed    is a student of Daffodil International University and pursuing a B.Sc. in the Electrical and Electronics Department. He passed from Government Bangabandhu college with a higher secondary. Microstrip patch antenna, terahertz antenna, and 5G application are some of his research interests. He can be contacted at email: sharif33-1152@diu.edu.bd.



Liton Chandra Paul    holds the position of Assistant Professor in the Electrical, Electronic, and Communication Engineering department at Pabna University of Science and Technology (PUST). He completed his Master's degree in Electrical and Electronic Engineering and Bachelor's degree in Electronics and Telecommunication Engineering at Rajshahi University of Engineering and Technology (RUET) in 2012 and 2015, respectively. During his academic journey, he actively participated in various non-profit social welfare organizations, making significant contributions to their endeavors. Currently, he is acting as an advisor for the IEEE PUST Student Branch, an advisor for the IEEE PUST AP-S SB Chapter, and a student activity coordinator for the IEEE APS-MTTS BD Joint Chapter. His research interests are RFIC, MIMO, machine learning, bio-electromagnetics, microwave technology, antennas, phased arrays, mmWave, metamaterials, absorber, metasurfaces, and wireless sensors. He can be contacted at email: litonpaule@gmail.com.